Supporting Information for ***Acta Phys. -Chim. Sin.*** doi: 10.3866/PKU.WHXB201805231

VO_{1-4}^{+} 阳离子与 *n*-C_mH_{2m+2} (*m* = 3, 5, 7) 烷烃的反应性研究：氧含量和碳链长度的影响

赵越 [1]，崔佳桐 [1]，胡继闯 [1,2]，马嘉壁 [1,*]

[1] 北京理工大学化学与化工学院，团簇科学重点实验室，北京 102488

[2] 上海卫星装备研究所，上海裕达实业有限公司，上海 200240

Reactivities of VO_{1-4}^{+} Toward *n*-C_mH_{2m+2} (*m* = 3, 5, 7) as Functions of Oxygen Content and Carbon Chain Length

ZHAO Yue [1], CUI Jiatong [1], HU Jichuang [1,2], MA Jiabi [*,1]

[1] Key Laboratory of Cluster Science, The Institute for Chemical Physics, School of Chemistry and Chemical Engineering, Beijing Institute of Technology, Beijing 102488, P. R. China.

[2] Shanghai Yuda Industrial Co., LTD., The Institute of Shanghai Spacecraft Equipment, Shanghai 200240, P. R. China.

[*]Corresponding authors. Email: majiabi@bit.edu.cn.

Contents:

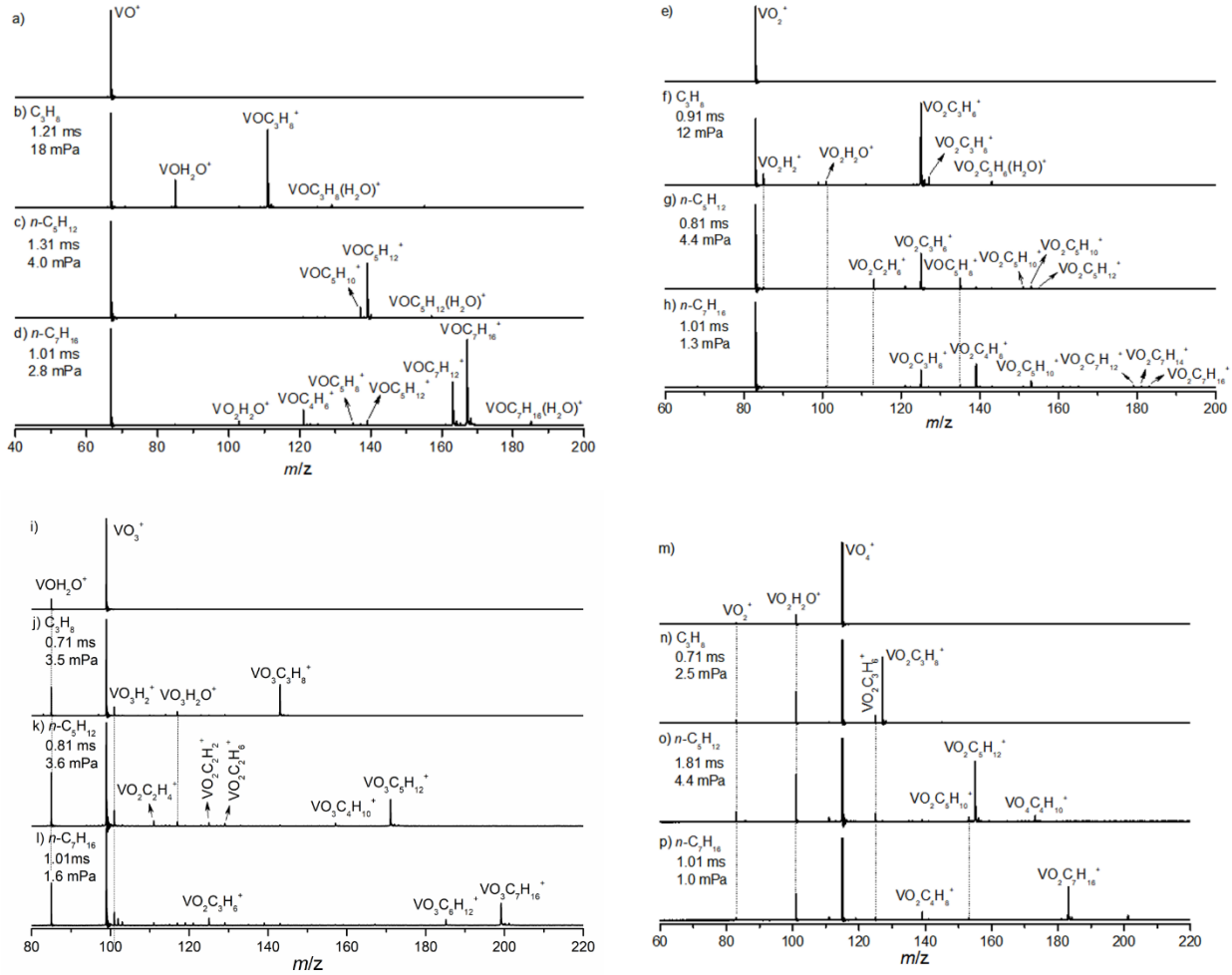

Fig. S1 TOF mass spectra for the reactions of mass-selected VO_{1-4}^+ cations (panels a, e, i, and m) with C_3H_8 (panels b, f, j, and n), n-C_5H_{12} (panels c, g, k, and o), and n-C_7H_{16} (panels d, h, l, and p). The reaction time and the C_3H_8, n-C_5H_{12}, and n-C_7H_{16} pressures are given, respectively.

Table S1 Products, Pseudo-First-Order Rate Coefficients (k), and Reaction Efficiencies (Φ) for the Reactions Investigated.

Reactions	Products/Equations		k_1 (cm^3 $molecule^{-1}$ s^{-1}) [a]/ Φ
$VO^+ + C_3H_8$	$VOC_3H_8^+$	100% (S1a)	/
	$VOC_7H_{16}^+$	42% (S2a)	
$VO^+ + n$-C_7H_{16}	$VOC_7H_{12}^+ + 2H_2$	38% (S2b)	1.27×10^{-9}/0.93
	Others	20% (S2c)	
	$VO_2C_3H_8^+$	50% (S3a)	
$VO_2^+ + C_3H_8$	$VO_2C_3H_6^+ + H_2$	49% (S3b)	6.54×10^{-10}/0.60
	$VO_2H_2^+ + C_3H_6$	1% (S3c)	
	$VO_2C_4H_8^+ + C_3H_8$	43% (S4a)	
	$VO_2C_3H_6^+ + C_4H_{10}$	28% (S4b)	
$VO_2^+ + n$-C_7H_{16}	$VO_2C_5H_{10}^+ + C_2H_6$	14% (S4c)	1.52×10^{-9}/1.18
	$VOC_5H_8^+ + C_2H_6O + H_2$	5% (S4d)	
	Others	10% (S4e)	

$VO_3^+ + C_3H_8$	$VO_3C_3H_8^+$	82%	(S5a)	4.79×10^{-10}/0.45
	$VO_3H_2^+ + C_3H_6$	18%	(S5b)	
$VO_3^+ + n\text{-}C_7H_{16}$	$VO_3C_7H_{16}^+$	62%	(S6a)	7.76×10^{-10}/0.63
	$VO_3H_2^+ + C_7H_{14}$	15%	(S6b)	
	$VO_3C_6H_2^+ + CH_4$	11%	(S6c)	
	$VO_2C_3H_6^+ + C_4H_{10}O$	10%	(S6d)	
	Others	2%	(S6e)	
$VO_4^+ + C_3H_8$	$VO_2C_3H_8^+ + O_2$	88%	(S7a)	1.21×10^{-9}/1.16
	$VO_2C_3H_6^+ + H_2 + O_2$	11%	(S7b)	
	Others	1%	(S7c)	
$VO_4^+ + n\text{-}C_7H_{16}$	$VO_2C_7H_{16} + O_2$	80%	(S8a)	2.23×10^{-9}/1.88
	$VO_2C_4H_8 + C_3H_8 + O_2$	12%	(S8b)	
	$VO_2C_3H_6 + C_4H_{10} + O_2$	3%	(S8c)	
	Others	5%	(S8d)	

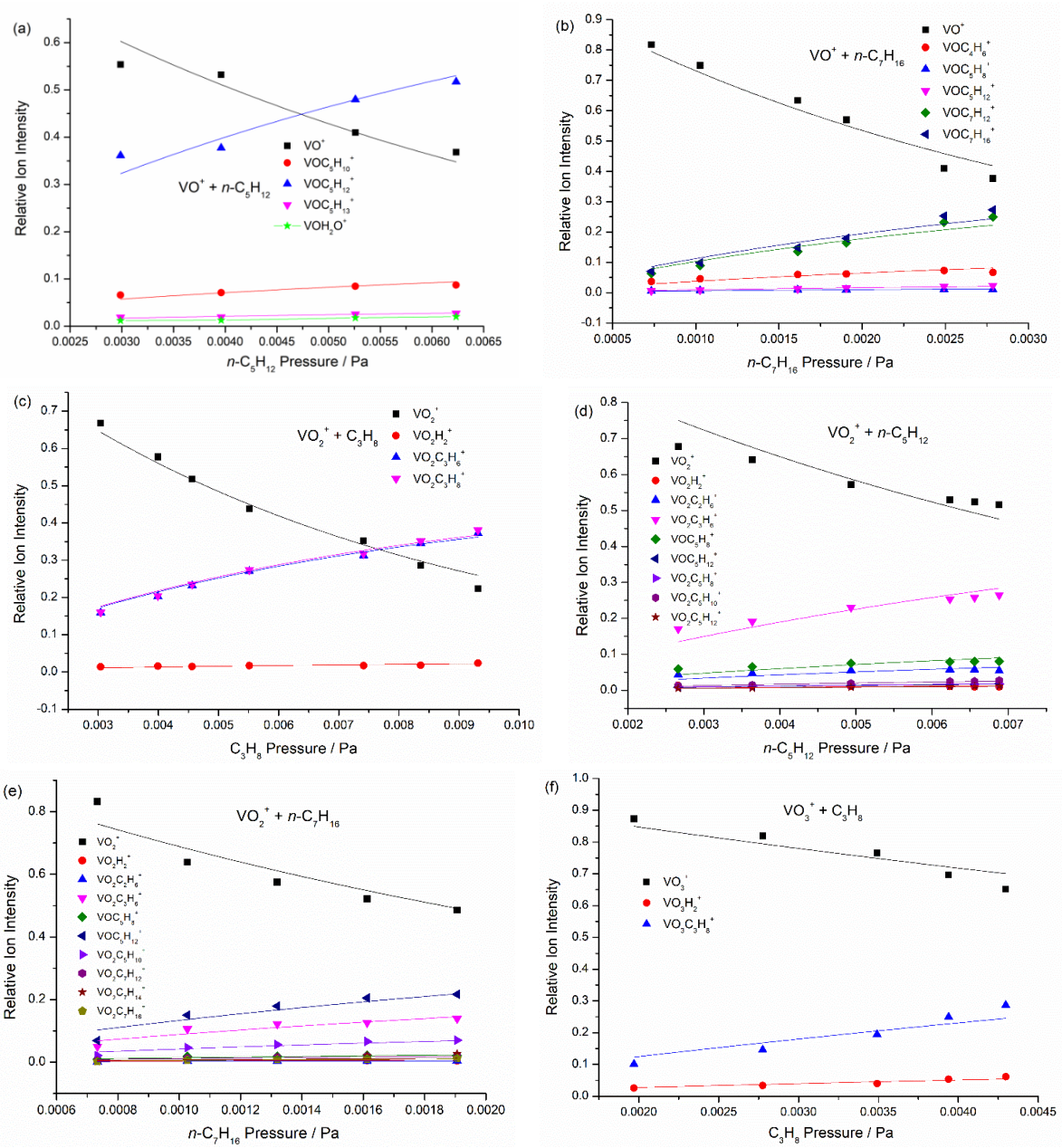

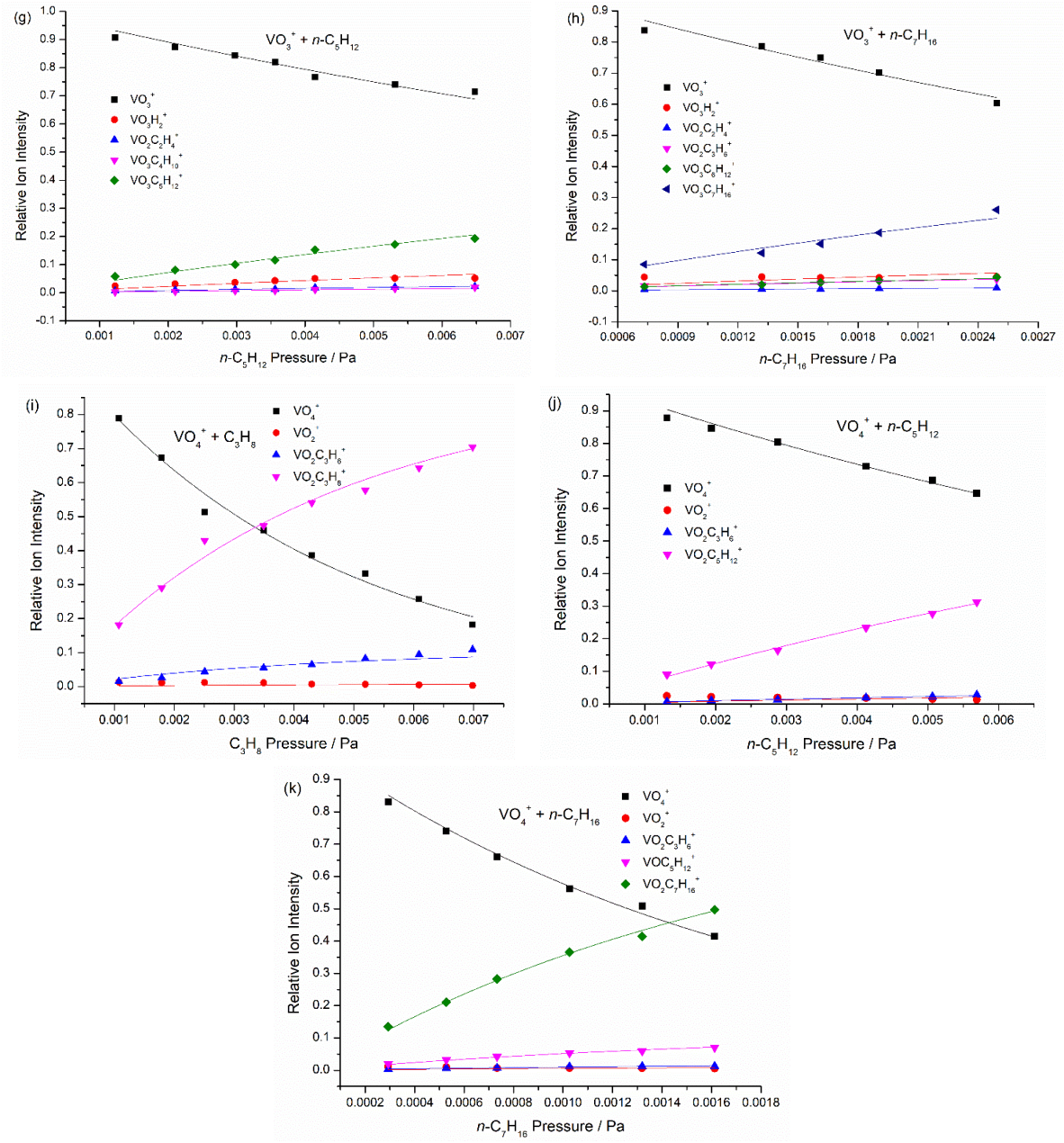

Fig. S2 Variations of the relative intensities of the reactant and product cations in the reactions between (a) VO^+ and *n*-C_5H_{12} with respect to the *n*-C_5H_{12} pressures for 1.3 ms, (b) VO^+ and *n*-C_7H_{16} with respect to the *n*-C_7H_{16} pressures for 1 ms, (c) VO_2^+ and C_3H_8 with respect to the C_3H_8 pressures for 1 ms, (d) VO_2^+ and *n*-C_5H_{12} with respect to the *n*-C_5H_{12} pressures for 0.8 ms, (e) VO_2^+ and *n*-C_7H_{16} with respect to the *n*-C_7H_{16} pressures for 1 ms, (f) VO_3^+ and C_3H_8 with respect to the C_3H_8 pressures for 0.8 ms, (g) VO_3^+ and *n*-C_5H_{12} with respect to the *n*-C_5H_{12} pressures for 0.8 ms, (h) VO_3^+ and *n*-C_7H_{16} with respect to the *n*-C_7H_{16} pressures for 1 ms, (i) VO_4^+ and C_3H_8 with respect to the C_3H_8 pressures for 0.8 ms, (j) VO_4^+ and *n*-C_5H_{12} with respect to the *n*-C_5H_{12} pressures for 0.8 ms, and (k) VO_4^+ and *n*-C_7H_{16} with respect to the *n*-C_7H_{16} pressures for 1 ms. The solid lines are fitted to the experimental data points derived with the approximation of the pseudo-first-order reaction mechanisms.

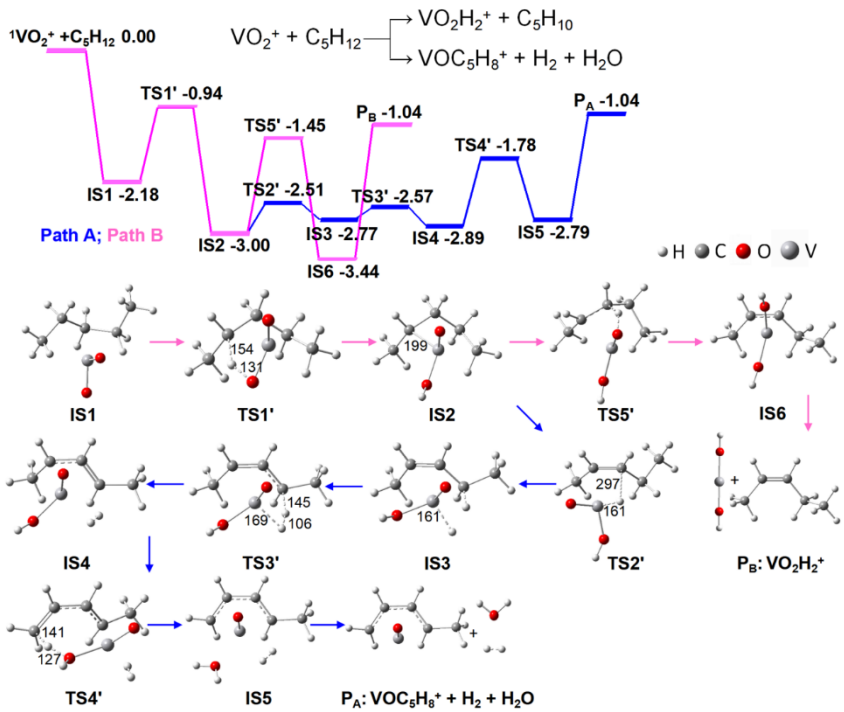

Fig. S3 DFT-calculated potential energy surface for the reaction of VO_2^+ with *n*-C_5H_{12}. Some bond lengths are given in pm. The zero-point vibration corrected energies ($\Delta H_{0\,K}$ in eV) of the reaction intermediates, transition states, and products with respect to the separated reactants are given. The superscripts indicate the spin states.

The PES of path from **IS1** to **IS2** is similar to that shown in Fig. 4 of the main text, which is not discussed herein. In path a, Intermediate **IS4** is formed involves two H atom transfer process through **IS2** → **TS2'** → **IS3** → **TS3'** → **IS4** and H_2 is generated. Through transition state **TS4'**, the HAT process happens with the generation of H_2O and yields intermediate **IS5**. Intermediate **IS5** further dissociates into $VOC_5H_8^+$ (**P_A**) under the evaporation of H_2 and H_2O with a barrier of 1.75 eV. In path b, through **IS1→TS1'→IS2→ TS5'→IS6**, two hydrogen atoms are successively transferred to two oxygen atoms, respectively. Intermediate **IS6** is formed and then dissociates into $VO_2H_2^+$ (**P_B**) and C_5H_{10}.

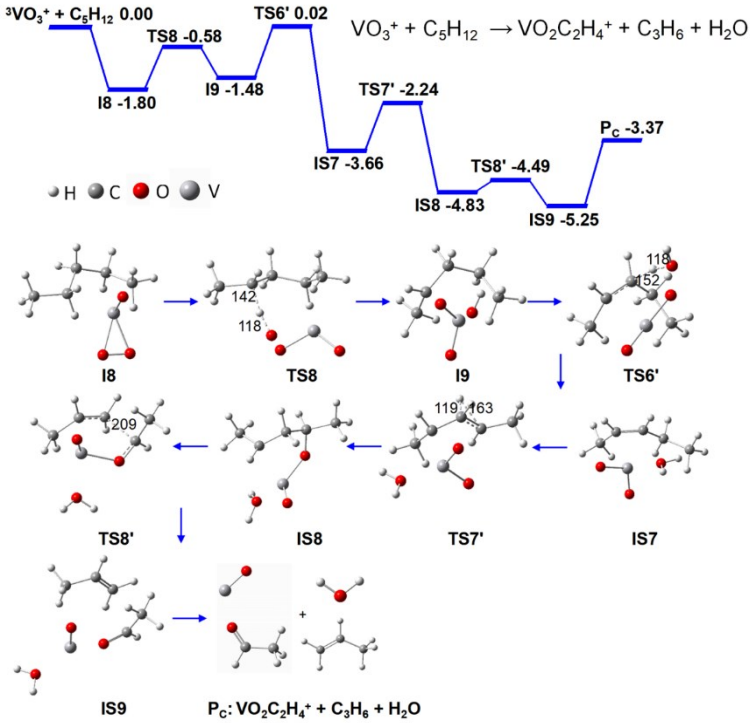

Fig. S4 DFT-calculated potential energy surface for the reaction of VO_3^+ with *n*-C_5H_{12}. Some bond lengths are given in pm. The zero-point vibration corrected energies ($\Delta H_{0\,K}$ in eV) of the reaction intermediates, transition states, and products with respect to the separated reactants are given. The superscripts indicate the spin states.

The PES of path from **I8** to **I9** is same as that shown in Fig. 5 of the main text, which is not discussed herein. As the HAT occurs, resulting in the formation of H_2O in intermediate **IS7** *via* **TS6'**. Then a H atom in **IS7** transfers from the methylene group to the C atom (**IS7** → **TS7'** → **IS8**), generating a C—O bond in the most stable structure (**IS8**). Through transition state **TS8'**, the C—C bond of intermediate **IS8** ruptures and yields intermediate **IS9**. Intermediate **IS9** has enough energy to dissociate into $VO_2C_2H_4^+$ (**P**C), C_3H_6 and H_2O.